PHARMACOLOGICAL INHIBITION OF INTEGRIN ALPHAV BETA3 AGGRAVATES EXPERIMENTAL LIVER FIBROSIS AND SUPPRESSES HEPATIC ANGIOGENESIS

E. Patsenker[1,2], **Y. Popov**[1,4], **F. Stickel**[2], **V. Schneider**[2], **M. Ledermann**[2], **H. Sägesser**[2], **G. Niedobitek**[1], **S. L. Goodman**[3], and **D. Schuppan**[1,4]

[1] Department of Medicine I, University of Erlangen-Nuernberg, Germany [2] Institute of Clinical Pharmacology and Visceral Research, University of Bern, Bern, Switzerland [3] Therapeutic area oncology Research, Merck KG, Darmstadt, Germany [4] Division of Gastroenterology, Beth Israel Deaconess Medical Center and Harvard Medical School, Boston MA, USA

Abstract

The vitronectin receptor integrin alpha v beta 3 (αvβ3) promotes angiogenesis by mediating migration and proliferation of endothelial cells, but also drives fibrogenic activation of hepatic stellate cells (HSC) in vitro. Expecting antifibrotic synergism, we studied the effect of αvβ3 inhibition in two in vivo models of liver fibrogenesis. Liver fibrosis was induced in rats by bile duct ligation (BDL) for 6 weeks or by thioacetamide (TAA) injections for 12 weeks. A specific αvβ3 (αvβ5) inhibitor (Cilengitide) was given i.p. twice daily at 15 mg/kg during BDL or after TAA-administration. Liver collagen was determined as hydroxyproline and gene expression was quantified by quantitative PCR. Liver angiogenesis, macrophage infiltration and hypoxia were assessed by CD31, CD68 and HIF-1α immunostaining.

Cilengitide decreased overall vessel formation. This was significant in portal areas of BDL and septal areas of TAA fibrotic rats, and was associated with a significant increase of liver collagen by 31% (BDL) and 27% (TAA), and upregulation of profibrogenic genes and matrix metalloproteinase-13. Treatment increased GGT in both models, while other serum markers remained unchanged. αvβ3 inhibition resulted in mild liver hypoxia, as evidenced by upregulation of hypoxia inducible genes. Liver infiltration by macrophages/Kupffer cells was not affected, although increases in TNF-α, IL-18 and COX-2 mRNA indicated modest macrophage activation.

Conclusion—Specific inhibition of integrin αvβ3 (αvβ5) *in vivo* decreased angiogenesis but worsened biliary (BDL) and septal (TAA) fibrosis, despite its antifibrogenic effect on HSC in vitro. Angiogenesis inhibitors should be used with caution in patients with hepatic fibrosis. (248 words).

Keywords

Angiogenesis; collagen; liver fibrosis; rat model; vitronectin receptor

INTRODUCTORY STATEMENT

Liver fibrosis is a typical complication of many chronic liver diseases and characterized by an excessive synthesis and deposition of extracellular matrix (ECM) that consists mainly of

Corresponding author: Detlef Schuppan, M.D., Ph.D., Division of Gastroenterology and Hepatology, Beth Israel Deaconess Medical Center and Harvard Medical School, Boston, MA 02215, phone: 617-6672371, fax: 617-6672767, dschuppan@bidmc.harvard.edu.

collagens, proteoglycans, and non-collagenous glycoproteins. (1) When damaged chronically, e.g. by viruses, autoimmunity or toxins like alcohol, the liver initiates a would healing reaction that results in hepatic fibrosis and cirrhosis. (2–4) The fibrogenic effector cells are activated hepatic stellate cells and (myo-) fibroblasts that proliferate and produce excess amounts of ECM components, which is unbalanced by fibrolysis. While mechanisms of hepatic fibrosis progression are fairly well understood, it remains a challenge to alter the balance of hepatic fibrogenesis and fibrolysis in favour of fibrolysis, and to develop safe and effective antifibrotic therapies for patients with chronic liver diseases.

The integrin αvβ3 is an adhesion receptor that is expressed mainly on endothelial cells (EC), but also on some tumor cells, HSC and inflammatory cells, especially monocytes and macrophages. (5–7) It plays an important role in EC migration, proliferation and blood vessel formation, and its dysregulation is involved in the pathogenesis of many diseases, especially of cancers, promoting metastasis and tumor-induced neovascularization. (8–10) Engagement of αvβ3 and its close relative αvβ5 upregulates ECM-degrading protease activities, such as that of matrix metalloprotease (MMP) -2, -3 and -9. (11–13) Small molecule inhibitors have been developed that suppress tumor angiogenesis in several animal experimental tumor models via inhibition of integrins αvβ3/αvβ5. (14–16)

Aberrant angiogenesis is clearly implicated in the progression of hepatic fibrosis and is considered a major determinant of hepatic dysfunction and irreversibility in cirrhosis. (3,17–19) However, results regarding the benefit of anti-angiogenic therapy in fibrosis are controversial. (20) Thus, in leptin-deficient Zucker rats fed with a choline-and amino acid-defined diet hepatic neovascularization was identified as a prerequisite for fibrosis progression, (21) and inhibition of new vessel growth by angiostatin or inhibitors of vascular endothelial growth factor (VEGF) in the CCl_4 model resulted in alleviation of liver fibrosis. (22,23) In contrast, in the remnant kidney model of progressive renal failure inhibition of angiogenesis worsened renal scaring, while application of proangiogenic VEGF reduced fibrosis and stabilized renal function. (24,25)

In order to assess the effect of antiangiogenic treatment in hepatic fibrosis, we selected Cilengitide (EMD121974), a specific inhibitor of integrins αvβ3 and αvβ5, that isused in human cancer studies. (26) Cilengitide was expected to be beneficial both due to its specific anti-angiogenic effect in vitro and in vivo (27,28) and to its antiproliferative and antifibrotic activity on HSC in vitro. (6) To allow more general conclusions, we chose two different animal models, secondary biliary fibrosis due to bile duct ligation (BDL) and panlobular fibrosis due to thioacetamide.

EXPERIMENTAL PROCEDURES

Materials

Cilengitide (EMD121974) was obtained from Merck (Darmstadt, Germany). Cilengitide (cyclo-Arg-Gly-Asp-D-Phe-(N-methyl)-Val) is an antagonist selective for integrins αvβ3 and αvβ5, with IC_{50} values of 3nM for αvβ3, 37nM for αvβ5, and 470nM for αvβ6 (29). Cilengitide was dissolved at 25mM in a pyrogen free solution of phosphate buffer (pH 6.0).

Animal experiments

Animal experiments were approved by the Government of Lower Franconia (permission No: 621.2531.31–20/00) and by the State-appointed Board on Animal Ethics, Switzerland (permission No: 105/04). Twenty male adult Wistar rats, weight 230–250g (Charles River, Sulzfeld, Germany), underwent a midline abdominal incision under ethylether anesthesia and cut of the common bile duct, which was doubly ligated with 5-0 silk (Perma-hand,

Ethicon, Germany). Six rats were sham-operated and served as controls. Cilengitide was given i.p. at 15mg/kg twice daily starting 1w after BDL (n=9). (30)

Thioacetamide (TAA) was applied at 200mg/kg twice per week for 12w. (31) One week after Cilengitide was given at 15mg/kg twice daily for 8w (n=8). Animals with TAA-induced fibrosis that remained untreated served as controls (n=7). Rats were sacrificed under ketamine anesthesia by exsanguination from the portal vein. Tissues were fixed in 4% formalin or snap frozen in liquid nitrogen for further analysis.

Hydroxyproline determination

Hydroxyproline (HYP) was determined biochemically from the left and right liver lobes (220–260mg) as described. (32)

Quantitative real-time PCR

150–200mg of tissue was homogenized in 1ml of RNApure (PeqLab, Erlangen, Germany). Total RNA was extracted and cDNA transcribed from 1μg of RNA according to the manufacturer's recommendation. Quantitative PCR was carried out on an ABI 7700 Sequence detector (Applied Biosystems, Rotkreuz, Switzerland). Probe and primer sets are shown in suppl. Table 1. β3 mRNA was quantified by real-time PCR using the SYBR green technique. Melting curve analysis and visualization of PCR-products was performed to ensure specificity of RT-PCR. For normalization the housekeeping genesβ2 microglobulin (β2MG) or glyceraldehyde 3-phosphate dehydrogenase (GAPDH) were amplified in a parallel reaction.

Liver histology

Tissue samples were fixed in formalin and embedded in paraffin using standard histological procedures. 3μm paraffin sections were stained with hematoxylin and eosin (H&E), and Sirius Red. (32,33) Thickness of fibrotic septa was measured as the width of the connective tissue separating cirrhotic nodules taken in the middle of the fibrotic bands at ×200 magnification and expressed as micrometers (Metamorph software computer-assisted analysis (MDS Analytical Technologies GmbH, Ismaning, Germany); 10 randomly selected septa were measured for each specimen. (34) Scoring was performed without prior knowledge of treatment.

Immunohistochemistry

Acetone-fixed frozen sections were incubated with 0.6% hydrogen peroxide (Merck, Darmstadt, Germany) for 30min. After blocking with 5% BSA the sections were incubated with monoclonal anti-CD31 (Fitzgerald, Concord MA, USA), monoclonal anti-CD68 (Serotec, Düsseldorf, Germany) (1:100), or monoclonal anti-HIF-1α (Abcam, Cambridge, UK) overnight at 4°C, followed by secondary goat anti-mouse peroxidase-labeled IgG (1:200) for 45min at RT and incubation with chromogenic substrate (Dako, Glostrup, Denmark) for 15min. Sections were counterstained with Mayer's Hemalaun and mounted in aqueous mounting medium (Dako, Glostrup, Denmark). Microvessel density (MVD) was assessed by counting the number of CD31 positive vessels using light microscopy, as described. (35) Four areas from each sample were quantified. Every CD31 positive endothelial cell or endothelial cell cluster that was clearly separated from adjacent microvessels was counted as a single countable vessel. Macrophage quantification was done by morphometrical analysis from 5 fields of every slide using Metamorph software and expressed as total area count of positive cells (magnification 40x).

Protein extraction and Western Blot analysis were performed as described. (6) 20μg of tissue lysates were applied to a 12% SDS-polyacrylamide gel, transferred to nitrocellulose

and blocked with 5% BSA. Anti-CD68 monoclonal antibody (Serotec, Kidlington, UK) was applied at a 1:100 dilution overnight at +4°C, following by incubation with horseradish peroxidase-conjugated goat anti-mouse antibody (1:2000). Immunodetected proteins were visualized using enhanced chemiluminescence (Amersham Biosciences, Freiburg, Germany).

Serum parameters

Alanine aminotransferase (ALT), aspartate aminotransferase (AST), alkaline phosphatase (ALP), gamma glutamyltransferase (GGT) and bilirubin were measured by the clinical chemical department of the University hospitals in Erlangen and Bern using kits from Boehringer (Mannheim, Germany) and an automated analyzer (BM/Hitachi 717).

Detection of apoptotic bodies

Apoptotic cells were identified by routine histological H&E staining, based on characteristic morphological features as assessed by an expert pathologist (GN). The apoptotic index was calculated as the number of apoptotic cells per 10 high power fields (hpf) from each liver section.

Statistical analysis

Statistical analyses were performed using Microsoft EXCEL software. Data are expressed as means ± SEM. The statistical significance of differences was evaluated using the unpaired Student's *t*-test.

RESULTS

The β3 subunit of integrin αvβ3 is highly expressed in rat liver

In normal rats, the highest basal expression of β3 integrin mRNA was found in liver when compared to spleen, muscle, heart, lungs and kidneys (Fig.1A). After bile duct ligation for 1, 3 and 6 weeksβ3 transcripts were upregulated time-dependently 1.2-, 2.2-, and 3.1-fold, respectively (Fig.1B). Upregulation in TAA-induced fibrosis was not significant (not shown), but this could be due to harvest of livers 1 week after the last dose of TAA, as compared to ongoing liver damage in the BDL model.

Liver histology of fibrotic animals with and without Cilengitide treatment

Rats with BDL for 6 weeks displayed marked bile duct proliferation with periductular collagen accumulation and incipient disruption of the lobular liver architecture (Fig.1C). This was accompanied by a mild to moderate inflammatory infiltrate consisting of lymphoid cells and macrophages. These histological parameters were not changed by Cilengitide (Fig. 1D). The numbers of apoptotic bodies reached 0.25 per 10 high power fields for the normal control livers, 8.5 in the untreated BDL animals, and 9.6 in the BDL animals treated with Cilengitide (not shown).

Twelve weeks of TAA, followed by 8 weeks of no treatment or treatment with Cilengitide, resulted in micro-macronodular cirrhosis that was highly populated by myofibroblasts. (Fig. 1E,F).

Cilengitide worsens biliary and panlobular liver fibrosis

Eight weeks of treatment with Cilengitide resulted in a 2-fold increase of the width of the collagenous septa (p<0.05) when compared to the untreated TAA group (Fig.2A–C). In rats with BDL and TAA-induced liver fibrosis, treatment with Cilengitide increased relative collagen accumulation significantly by 31% and by 27%, respectively (Fig.2D), while the

increase of total liver collagen did not reach significance (Table 2). In BDL rats which received Cilengitide, the expression of profibrogenic genes (procollagen α1(I), TGFβ1, TIMP-1, TIMP-2, PDGFR-β, plasminogen activator inhibitor-1) and of potentially fibrolytic MMP-13 was significantly higher than in rats with BDL alone (Table 1A). αSMA, TGFβ2, PDGF-BB and CTGF transcripts showed only a trend of upregulation in the treated group. In TAA-induced fibrosis only procollagen α1(I) and TIMP-1 mRNA were significantly induced in the group that received Cilengitide (Table 1B).

Hepatic expression of proinflammatory cyclo-oxygenase-2 (COX-2), tumor necrosis factor-α (TNF-α) and IL-18 mRNA was strongly upregulated in both fibrosis models. Treatment with Cilengitide further induced COX-2, TNF-α and IL-18 in BDL rats by 1.6-, 2.3 and 1.4-fold, respectively, whereas in TAA-induced cirrhosis only IL-18 was 1.8-fold upregulated (p 0.05) Fig.2E,F.

Organ weights and serum parameters

Liver and spleen weights were significantly increased in rats with BDL and TAA-induced cirrhosis. These were not altered by Cilengitide treatment (Table 2A,B). Bile duct ligation and TAA administration resulted in a strong elevation of ALT, AST, ALP and bilirubin levels, but only GGT was further increased by Cilengitide: 4.7-fold in BDL and 2.3-fold in TAA model. (Table 2A,B).

Effect of Cilengitide on hepatic angiogenesis in rats with liver fibrosis

CD31 staining highlighted sinusoidal endothelial cells and endothelia of portal vessels and central veins in normal livers, whereas BDL animals showed an irregular vascular pattern in the portal/immediate periportal areas of the expanding portal tracts (Fig.3A–C). Treatment with Cilengitide resulted in inhibition of vessel formation by 25% in portal and periportal areas (p<0.05) (Fig.3D), but the total number of CD31 positive sinusoidal endothelial cells remained unchanged (Fig.3E). The number of vessels in portal tracts relative to hydroxyproline (mg per g of liver), reflecting the density of vessels in the fibrotic areas, was even more drastically reduced in Cilengitide-treated BDL rats (Fig.3F).

Rats with TAA-induced cirrhosis revealed prominent CD31 staining within fibrotic septa, with less prominent staining of sinusoids (Fig.4A–D), as compared to the stronger staining of sinusoids in BDL. Cilengitide treatment reduced overall vessel formation by 13% which did not reach statistical significance (p<0.1, Fig.4E). However, as for BDL the number of blood vessels in the fibrotic portal tracts and septa, as represented by their ratio to hydroxyproline was reduced significantly by Cilengitide (Fig.4F).

Hepatic macrophage infiltration is not affected by Cilengitide

Liver macrophages/Kupffer cells, important contributors to fibrosis progression or reversal, (36,37) also express functional integrin αvβ3 which modulates their migration and activation. (7) When compared to normal rat livers, macrophages increased about 3-fold in rats with BDL, and were mainly localized in the fibrotic tissue (Fig.5A–D). Treatment with Cilengitide did not affect macrophage numbers in both fibrosis models (Fig.5E,F). This was confirmed by CD68 Western blotting and densitometry(suppl. Fig.1A,B).

Cilengitide treatment induces mild liver hypoxia

Treatment with Cilengitide resulted in upregulation of hypoxia-induced HIF-1α transcripts and protein, and the HIF-1α dependent genes VEGF, iNOS and EPO in the BDL model. In the TAA model only VEGF mRNA was upregulated significantly (by 24%) and EPO mRNA was undetectable (Fig.6, suppl. Fig.2).

DISCUSSION

The role of neovascularization in the liver during fibrosis progression is controversial. In a number of studies, enhanced angiogenesis was associated with faster fibrosis progression (19–21,23,38), while in the remnant kidney model neoangiogenesis was associated with lessened fibrosis. (24,25) We chose validated models of biliary (BDL) and panlobular (TAA) fibrosis, in order to assess the antifibrotic effect of a specific small molecule inhibitor for the related integrins $\alpha v\beta 3$ and $\alpha v\beta 5$ (EMD121974 or Cilengitide), both being expressed on endothelial cells (14,39), and $\alpha v\beta 3$ being found on macrophages and activated HSC (6,7,40). A dual benefit was expected, since activated HSC and myofibroblasts, the major profibrogenic effector cells in the liver, which when blocked by Cilengitide lead to downregulation of several profibrogenic genes and complete inhibition of HSC migration, resulting in a fibrolytic phenotype, characterized by enhanced expression and activity of certain MMPs. (6) Of note, Cilengitide has demonstrated biological activity in vivo, i.e., antitumor activity in colorectal carcinoma, melanoma and other cancers. (41) Furthermore, our preliminary screening of $\alpha v\beta 3$ integrin expression in different organs of healthy rats unraveled particularly high levels of expression in the liver, followed by lung and spleen, and subsequent to bile duct ligation in rats, hepatic expression of the $\beta 3$ subunit was markedly upregulated and correlated with the stage of fibrosis.

In contrast to the expected antifibrotic effect on HSC in vitro, in vivo Cilengitide worsened liver fibrosis, either when given during progression of biliary fibrosis (BDL) or for established TAA-induced fibrosis/cirrhosis. This was accompanied by an increase in procollagen $\alpha 1(I)$, TGF$\beta 1$, αSMA, TIMP-1, PDGFR-β and PAI-1 transcripts as compared to untreated fibrotic animals. Furthermore, MMP-13 mRNA, was upregulated, as previously observed in HSC in vitro. (6) If an upregulation of MMP-13 reflects fibrolysis or merely increased ECM turnover during fibrogenesis remains unresolved. Serum markers of liver damage, such as ALT, AST and ALP were not affected by Cilengitide in both models, except for an increase of GGT, possibly due to hypoxic damage to bile duct epithelia. Similarly, spleen weight which can be considered an indirect and crude indicator of portal hypertension (42) was not affected by anti-angiogenic treatment in both fibrosis models.

Hepatic transcripts of COX-2, TNF-α, IL-18 and iNOS, effectors of inflammation that are mainly produced by macrophages/Kupffer cells (43), were induced in Cilengitide-treated rats with BDL and less strikingly with TAA-induced fibrosis, whereas macrophage numbers remained unaffected. An important role of the $\alpha v\beta 3$ integrin in dampening (macrophage-induced) inflammation (44) and in suppression of hyperlipidemia-induced vascular inflammation (45) was recently shown. This suggests that by blocking $\alpha v\beta 3$ integrin, Cilengitide mildly increased macrophage activation and the release of inflammatory mediators. Taken together, in contrast to the beneficial antifibrotic *in vitro* effects on isolated HSC, (6,40) *in vivo* inhibition of integrins $\alpha v\beta 3$ and $\alpha v\beta 5$ promoted hepatic inflammation and fibrogenesis. Apart from the mild pro-inflammatory effect of $\alpha v\beta 3$ inhibition on macrophages/Kupffer the relative loss of portal and septal but not sinusoidal endothelial cells and vessels may have contributed to liver fibrosis progression. Thus inhibition of activated endothelial cells in the expanding portal areas could have worsened fibrogenesis as a consequence of hepatic hypoxia. A lack of supplying blood vessels can compromise oxygen and nutrient delivery to the liver parenchyma, with subsequently enhanced oxidative stress and pro-inflammatory responses, (46,47) and significant hypoxia was found throughout the hepatic lobule in >95% of hepatocytes after 2 weeks of BDL. (48) This assumption is supported by the induction of hypoxia-inducible genes by Cilengitide, such as HIF-1α, VEGF, iNOS and EPO, predominantly in the BDL model in which the antagonist also induced a more rigorous fibrogenic response as compared to the TAA model.

Our findings are in accordance with observations that angiogenesis inhibition promoted renal interstitial fibrosis. (20,48) Furthermore, several investigations showed that hepatocellular hypoxia and angiogenesis went hand in hand with fibrogenesis after liver injury and that hypoxia directly contributed to the progression of liver fibrosis. Thus, hypoxia in vitro induced the expression of procollagen α1(I), VEGF and its receptors in activated HSC, and of VEGF in hepatocytes. (49) Similarly, in CCl_4-induced cirrhosis hypoxia lead to an upregulation of TGFβ1 expression in hepatocytes. (50) Finally, pro-angiogenic intervention, i.e., therapy with endothelial progenitor cells ameliorated fibrosis and improved survival following CCl_4-induced liver injury in mice via promotion of parenchymal liver regeneration. (51,52)

Our results contrast with a recent study that demonstrated that (antiangiogenic) treatment with the multikinase inhibitor Sunitinib ameliorated the inflammatory infiltrate, fibrosis and portal pressure of rats with CCl_4-induced fibrosis. (53) The discrepant results could be explained by the different models used, the much shorter treatment with Sunitinib (only 1 week vs 5 and 8 weeks in our studies), and the different molecular targets. Of note, Sunitinib mainly inhibits VEGF and PDGF receptors, but also a spectrum of other receptor tyrosin kinases (c-kit, RET, G-CSF, Flt3). PDGF-AB or -BB, activating the PDGFR-β, is considered a profibrogenic growth factor due to its promigratory and proproliferative action on HSC (54), and inhibition of the PDGFR-β on HSC with Imatinib blocked early but not advanced hepatic fibrogenesis. (55)

In summary, antiangiogenic therapy via pharmacological inhibition of αvβ3 (and αvβ5) integrin promoted fibrosis progression both in experimental biliary (portal) and panlobular hepatic fibrosis, despite clear antifibrotic effects of such inhibition on isolated HSC which upregulate this receptor upon activation. This indicates that liver neoangiogenesis mediated via integrins αvβ3 (and αvβ5) exerts beneficial antifibrotic activities during or after chronic liver damage, outweighing their profibrogenic role in HSC in vitro. Our data also suggest a note of caution for the use of potent and specific antiangiogenic substances in tumor patients with hepatic fibrogenesis, or for the treatment of liver fibrosis itself.

Supplementary Material

Refer to Web version on PubMed Central for supplementary material.

Acknowledgments

List of abbreviations

Cil	Cilengitide
CTGF	connective tissue growth factor
COX-2	cyclooxygenase-2
ECM	extracellular matrix
iNOS	inducible nitric oxide synthase
HIF-1α	hypoxia-inducible factor-1α

HSC	hepatic stellate cell
HYP	hydroxyproline
MMP	matrix metalloproteinase
PDGF	platelet derived growth factor
TGFβ	transforming growth factor β
TIMP	tissue inhibitor of matrix metalloproteinases

References

1. Schuppan D, Ruehl M, Somasundaram R, Hahn EG. Matrix as a modulator of hepatic fibrogenesis. Semin Liver Dis. 2001; 21:351–372. [PubMed: 11586465]

2. Bataller R, Brenner DA. Liver fibrosis. J Clin Invest. 2005; 115:209–218. [PubMed: 15690074]

3. Schuppan D, Afdhal NH. Liver cirrhosis. Lancet. 2008; 371:838–851. [PubMed: 18328931]

4. Friedman SL. Mechanisms of hepatic fibrogenesis. Gastroenterology. 2008; 134:1655–1669. [PubMed: 18471545]

5. Hood JD, Cheresh DA. Role of integrins in cell invasion and migration. Nat Rev Cancer. 2002; 2:91–100. [PubMed: 12635172]

6. Patsenker E, Popov Y, Wiesner M, Goodman SL, Schuppan D. Pharmacological inhibition of the vitronectin receptor abrogates PDGF-BB-induced hepatic stellate cell migration and activation in vitro. J Hepatol. 2007; 46:878–887. [PubMed: 17258347]

7. Chung AS, Gao Q, Kao WJ. Either integrin subunit beta1 or beta3 is involved in mediating monocyte adhesion, IL-1beta protein and mRNA expression in response to surfaces functionalized with fibronectin-derived peptides. J Biomater Sci Polym Ed. 2007; 18:713–729. [PubMed: 17623553]

8. Sato T, Konishi K, Kimura H, Maeda K, Yabushita K, Tsuji M, Miwa A. Vascular integrin beta 3 and its relation to pulmonary metastasis of colorectal carcinoma. Anticancer Res. 2001; 21:643–647. [PubMed: 11299820]

9. Ruegg C, Mariotti A. Vascular integrins: pleiotropic adhesion and signaling molecules in vascular homeostasis and angiogenesis. Cell Mol Life Sci. 2003; 60:1135–1157. [PubMed: 12861381]

10. Mahabeleshwar GH, Feng W, Phillips DR, Byzova TV. Integrin signaling is critical for pathological angiogenesis. J Exp Med. 2006; 203:2495–2507. [PubMed: 17030947]

11. Bendeck MP, Irvin C, Reidy M, Smith L, Mulholland D, Horton M, Giachelli CM. Smooth muscle cell matrix metalloproteinase production is stimulated via alpha(v)beta(3) integrin. Arterioscler Thromb Vasc Biol. 2000; 20:1467–1472. [PubMed: 10845859]

12. Jackson C. Matrix metalloproteinases and angiogenesis. Curr Opin Nephrol Hypertens. 2002; 11:295–299. [PubMed: 11981259]

13. Baum O, Hlushchuk R, Forster A, Greiner R, Clezardin P, Zhao Y, Djonov V, et al. Increased invasive potential and up-regulation of MMP-2 in MDA-MB-231 breast cancer cells expressing the beta3 integrin subunit. Int J Oncol. 2007; 30:325–332. [PubMed: 17203213]

14. Belvisi L, Riccioni T, Marcellini M, Vesci L, Chiarucci I, Efrati D, Potenza D, et al. Biological and molecular properties of a new alpha(v)beta3/alpha(v)beta5 integrin antagonist. Mol Cancer Ther. 2005; 4:1670–1680. [PubMed: 16275988]

15. Harms JF, Welch DR, Samant RS, Shevde LA, Miele ME, Babu GR, Goldberg SF, et al. A small molecule antagonist of the alpha(v)beta3 integrin suppresses MDA-MB-435 skeletal metastasis. Clin Exp Metastasis. 2004; 21:119–128. [PubMed: 15168729]

16. Zhao Y, Bachelier R, Treilleux I, Pujuguet P, Peyruchaud O, Baron R, Clement-Lacroix P, et al. Tumor alphavbeta3 integrin is a therapeutic target for breast cancer bone metastases. Cancer Res. 2007; 67:5821–5830. [PubMed: 17575150]

17. Friedman SL, Bansal MB. Reversal of hepatic fibrosis -- fact or fantasy? Hepatology. 2006; 43:S82–88. [PubMed: 16447275]

18. Desmet VJ, Roskams T. Cirrhosis reversal: a duel between dogma and myth. J Hepatol. 2004; 40:860–867. [PubMed: 15094237]

19. Taura K, De Minicis S, Seki E, Hatano E, Iwaisako K, Osterreicher CH, Kodama Y, et al. Hepatic stellate cells secrete angiopoietin 1 that induces angiogenesis in liver fibrosis. Gastroenterology. 2008; 135:1729–1738. [PubMed: 18823985]

20. Kang DH, Johnson RJ. Vascular endothelial growth factor: a new player in the pathogenesis of renal fibrosis. Curr Opin Nephrol Hypertens. 2003; 12:43–49. [PubMed: 12496665]

21. Kitade M, Yoshiji H, Kojima H, Ikenaka Y, Noguchi R, Kaji K, Yoshii J, et al. Leptin-mediated neovascularization is a prerequisite for progression of nonalcoholic steatohepatitis in rats. Hepatology. 2006; 44:983–991. [PubMed: 17006938]

22. Vogten JM, Drixler TA, te Velde EA, Schipper ME, van Vroonhoven TJ, Voest EE, Borel Rinkes IH. Angiostatin inhibits experimental liver fibrosis in mice. Int J Colorectal Dis. 2004; 19:387–394. [PubMed: 14716496]

23. Yoshiji H, Kuriyama S, Yoshii J, Ikenaka Y, Noguchi R, Hicklin DJ, Wu Y, et al. Vascular endothelial growth factor and receptor interaction is a prerequisite for murine hepatic fibrogenesis. Gut. 2003; 52:1347–1354. [PubMed: 12912869]

24. Kang DH, Hughes J, Mazzali M, Schreiner GF, Johnson RJ. Impaired angiogenesis in the remnant kidney model: II. Vascular endothelial growth factor administration reduces renal fibrosis and stabilizes renal function. J Am Soc Nephrol. 2001; 12:1448–1457. [PubMed: 11423573]

25. Kang DH, Joly AH, Oh SW, Hugo C, Kerjaschki D, Gordon KL, Mazzali M, et al. Impaired angiogenesis in the remnant kidney model: I. Potential role of vascular endothelial growth factor and thrombospondin-1. J Am Soc Nephrol. 2001; 12:1434–1447. [PubMed: 11423572]

26. Hariharan S, Gustafson D, Holden S, McConkey D, Davis D, Morrow M, Basche M, et al. Assessment of the biological and pharmacological effects of the alpha nu beta3 and alpha nu beta5 integrin receptor antagonist, cilengitide (EMD 121974), in patients with advanced solid tumors. Ann Oncol. 2007; 18:1400–1407. [PubMed: 17693653]

27. Cai W, Chen X. Anti-angiogenic cancer therapy based on integrin alphavbeta3 antagonism. Anticancer Agents Med Chem. 2006; 6:407–428. [PubMed: 17017851]

28. Reardon DA, Nabors LB, Stupp R, Mikkelsen T. Cilengitide: an integrin-targeting arginine-glycine-aspartic acid peptide with promising activity for glioblastoma multiforme. Expert Opin Investig Drugs. 2008; 17:1225–1235.

29. Goodman SL, Holzemann G, Sulyok GA, Kessler H. Nanomolar small molecule inhibitors for alphav(beta)6, alphav(beta)5, and alphav(beta)3 integrins. J Med Chem. 2002; 45:1045–1051. [PubMed: 11855984]

30. Eskens FA, Dumez H, Hoekstra R, Perschl A, Brindley C, Bottcher S, Wynendaele W, et al. Phase I and pharmacokinetic study of continuous twice weekly intravenous administration of Cilengitide (EMD 121974), a novel inhibitor of the integrins alphavbeta3 and alphavbeta5 in patients with advanced solid tumours. Eur J Cancer. 2003; 39:917–926. [PubMed: 12706360]

31. Popov Y, Patsenker E, Bauer M, Niedobitek E, Schulze-Krebs A, Schuppan D. Halofuginone induces matrix metalloproteinases in rat hepatic stellate cells via activation of p38 and NFkappaB. J Biol Chem. 2006; 281:15090–15098. [PubMed: 16489207]

32. Popov Y, Patsenker E, Fickert P, Trauner M, Schuppan D. Mdr2 (Abcb4)−/− mice spontaneously develop severe biliary fibrosis via massive dysregulation of pro- and antifibrogenic genes. J Hepatol. 2005; 43:1045–1054. [PubMed: 16223543]

33. Patsenker E, Popov Y, Stickel F, Jonczyk A, Goodman SL, Schuppan D. Inhibition of integrin alphavbeta6 on cholangiocytes blocks transforming growth factor-beta activation and retards biliary fibrosis progression. Gastroenterology. 2008; 135:660–670. [PubMed: 18538673]

34. Fabris L, Cadamuro M, Guido M, Spirli C, Fiorotto R, Colledan M, Torre G, et al. Analysis of liver repair mechanisms in Alagille syndrome and biliary atresia reveals a role for notch signaling. Am J Pathol. 2007; 171:641–653. [PubMed: 17600123]

35. Foss AJ, Alexander RA, Jefferies LW, Hungerford JL, Harris AL, Lightman S. Microvessel count predicts survival in uveal melanoma. Cancer Res. 1996; 56:2900–2903. [PubMed: 8674036]

36. Duffield JS, Forbes SJ, Constandinou CM, Clay S, Partolina M, Vuthoori S, Wu S, et al. Selective depletion of macrophages reveals distinct, opposing roles during liver injury and repair. J Clin Invest. 2005; 115:56–65. [PubMed: 15630444]

37. Fallowfield JA, Mizuno M, Kendall TJ, Constandinou CM, Benyon RC, Duffield JS, Iredale JP. Scar-associated macrophages are a major source of hepatic matrix metalloproteinase-13 and facilitate the resolution of murine hepatic fibrosis. J Immunol. 2007; 178:5288–5295. [PubMed: 17404313]

38. Yoshiji H, Kuriyama S, Fukui H. Angiotensin-I-converting enzyme inhibitors may be an alternative anti-angiogenic strategy in the treatment of liver fibrosis and hepatocellular carcinoma. Possible role of vascular endothelial growth factor. Tumour Biol. 2002; 23:348–356. [PubMed: 12677092]

39. Maubant S, Saint-Dizier D, Boutillon M, Perron-Sierra F, Casara PJ, Hickman JA, Tucker GC, et al. Blockade of alpha v beta3 and alpha v beta5 integrins by RGD mimetics induces anoikis and not integrin-mediated death in human endothelial cells. Blood. 2006; 108:3035–3044. [PubMed: 16835373]

40. Zhou X, Murphy FR, Gehdu N, Zhang J, Iredale JP, Benyon RC. Engagement of alphavbeta3 integrin regulates proliferation and apoptosis of hepatic stellate cells. J Biol Chem. 2004; 279:23996–24006. [PubMed: 15044441]

41. Raguse JD, Gath HJ, Bier J, Riess H, Oettle H. Cilengitide (EMD 121974) arrests the growth of a heavily pretreated highly vascularised head and neck tumour. Oral Oncol. 2004; 40:228–230. [PubMed: 14693249]

42. Hoefs JC, Wang FW, Lilien DL, Walker B, Kanel G. A novel, simple method of functional spleen volume calculation by liver-spleen scan. J Nucl Med. 1999; 40:1745–1755. [PubMed: 10520718]

43. Nanji AA, Miao L, Thomas P, Rahemtulla A, Khwaja S, Zhao S, Peters D, et al. Enhanced cyclooxygenase-2 gene expression in alcoholic liver disease in the rat. Gastroenterology. 1997; 112:943–951. [PubMed: 9041257]

44. Ren J, Avery J, Zhao H, Schneider JG, Ross FP, Muslin AJ. Beta3 integrin deficiency promotes cardiac hypertrophy and inflammation. J Mol Cell Cardiol. 2007; 42:367–377. [PubMed: 17184791]

45. Schneider JG, Zhu Y, Coleman T, Semenkovich CF. Macrophage beta3 integrin suppresses hyperlipidemia-induced inflammation by modulating TNFalpha expression. Arterioscler Thromb Vasc Biol. 2007; 27:2699–2706. [PubMed: 17951320]

46. Horie Y, Wolf R, Russell J, Shanley TP, Granger DN. Role of Kupffer cells in gut ischemia/reperfusion-induced hepatic microvascular dysfunction in mice. Hepatology. 1997; 26:1499–1505. [PubMed: 9397990]

47. Siegmund SV, Brenner DA. Molecular pathogenesis of alcohol-induced hepatic fibrosis. Alcohol Clin Exp Res. 2005; 29:102S–109S. [PubMed: 16344593]

48. Rosmorduc O, Wendum D, Corpechot C, Galy B, Sebbagh N, Raleigh J, Housset C, et al. Hepatocellular hypoxia-induced vascular endothelial growth factor expression and angiogenesis in experimental biliary cirrhosis. Am J Pathol. 1999; 155:1065–1073. [PubMed: 10514389]

49. Corpechot C, Barbu V, Wendum D, Kinnman N, Rey C, Poupon R, Housset C, et al. Hypoxia-induced VEGF and collagen I expressions are associated with angiogenesis and fibrogenesis in experimental cirrhosis. Hepatology. 2002; 35:1010–1021. [PubMed: 11981751]

50. Jeong WI, Do SH, Yun HS, Song BJ, Kim SJ, Kwak WJ, Yoo SE, et al. Hypoxia potentiates transforming growth factor-beta expression of hepatocyte during the cirrhotic condition in rat liver. Liver Int. 2004; 24:658–668. [PubMed: 15566519]

51. Ueno T, Nakamura T, Torimura T, Sata M. Angiogenic cell therapy for hepatic fibrosis. Med Mol Morphol. 2006; 39:16–21. [PubMed: 16575510]

52. Taniguchi E, Kin M, Torimura T, Nakamura T, Kumemura H, Hanada S, Hisamoto T, et al. Endothelial progenitor cell transplantation improves the survival following liver injury in mice. Gastroenterology. 2006; 130:521–531. [PubMed: 16472604]

53. Tugues S, Fernandez-Varo G, Munoz-Luque J, Ros J, Arroyo V, Rodes J, Friedman SL, et al. Antiangiogenic treatment with sunitinib ameliorates inflammatory infiltrate, fibrosis, and portal pressure in cirrhotic rats. Hepatology. 2007; 46:1919–1926. [PubMed: 17935226]

54. Pinzani M, Gesualdo L, Sabbah GM, Abboud HE. Effects of platelet-derived growth factor and other polypeptide mitogens on DNA synthesis and growth of cultured rat liver fat-storing cells. J Clin Invest. 1989; 84:1786–1793. [PubMed: 2592560]

55. Neef M, Ledermann M, Saegesser H, Schneider V, Widmer N, Decosterd LA, Rochat B, et al. Oral imatinib treatment reduces early fibrogenesis but does not prevent progression in the long term. J Hepatol. 2006; 44:167–175. [PubMed: 16168515]
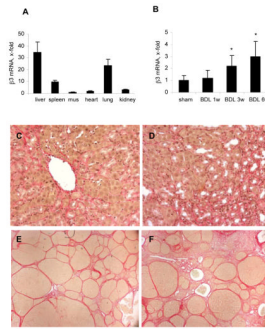
Fig.1. Levels of β3 integrin mRNA and hepatic collagen deposition in untreated and Cilengitide-treated rats with experimental liver fibrosis

(**A**) Integrin β3 mRNA in different organs of normal rats; (**B**) hepatic β3 mRNA after 1, 3 and 6w of BDL. Transcripts were measured by real-time PCR, normalized to β2MG and expressed as x-fold change vs the corresponding control (means±SD). Sirius Red staining of livers from rats with: (**C**) BDL 6w (n=8); (**D**) BDL 6w + Cilengitide 30mg/kg/day for 5w (n=9); (**E**) TAA fibrosis and spontaneous reversal (TAA-R: TAA 12w + 8w of recovery, n=7); (**F**) TAA-R + Cilengitide 30mg/kg/day for 8w (n=8). Shown are representative images (magnification 40x).
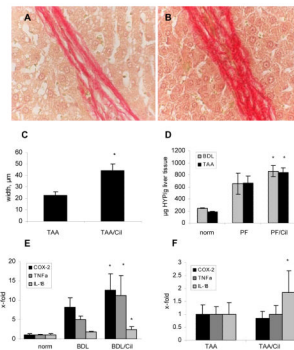
Fig.2. Hepatic collagen content, septal thickness and inflammation markers of fibrotic animals untreated or treated with Cilengitide

The thickness of fibrotic septa was measured in rats with TAA-induced fibrosis (**A**) without (TAA-R) and (**B**) with (TAA-R + Cil) Cilengitide treatment (magnification 100x); (**C**) Quantification of mid-septal thickness measured with Metamorph software (μm); (**D**) Relative hepatic hydroxyproline (mg/g of wet liver); (**E,F**) macrophage activation markers COX-2, TNF-α and IL-18 in all experimental groups (means±SD). *p<0.05 vs the untreated fibrosis control.

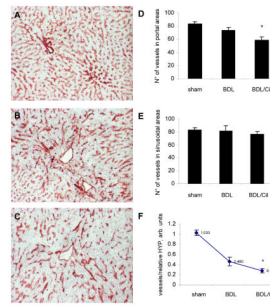**Fig.3. CD31 immunohistochemistry of bile duct ligated rats treated with/without Cilengitide**
(**A**) Sham-operated (n=4); (**B**) BDL 6w (n=8); (**C**) BDL 6w + Cilengitide 30mg/kg/day 5w
(n=9). Quantification of angiogenesis in portal areas (**D**) and in sinusoidal areas (**E**) of all
experimental groups. Calculation of CD31-positive vessels was performed in four areas
from each liver section using light microscopy (magnification 10x) and is expressed as a
number of vessels per field (means±SD); (**F**) Vessel number per fibrotic area is calculated as
the ratio of portal vessels to relative HYP (means±SD); *p<0.05 vs BDL alone.
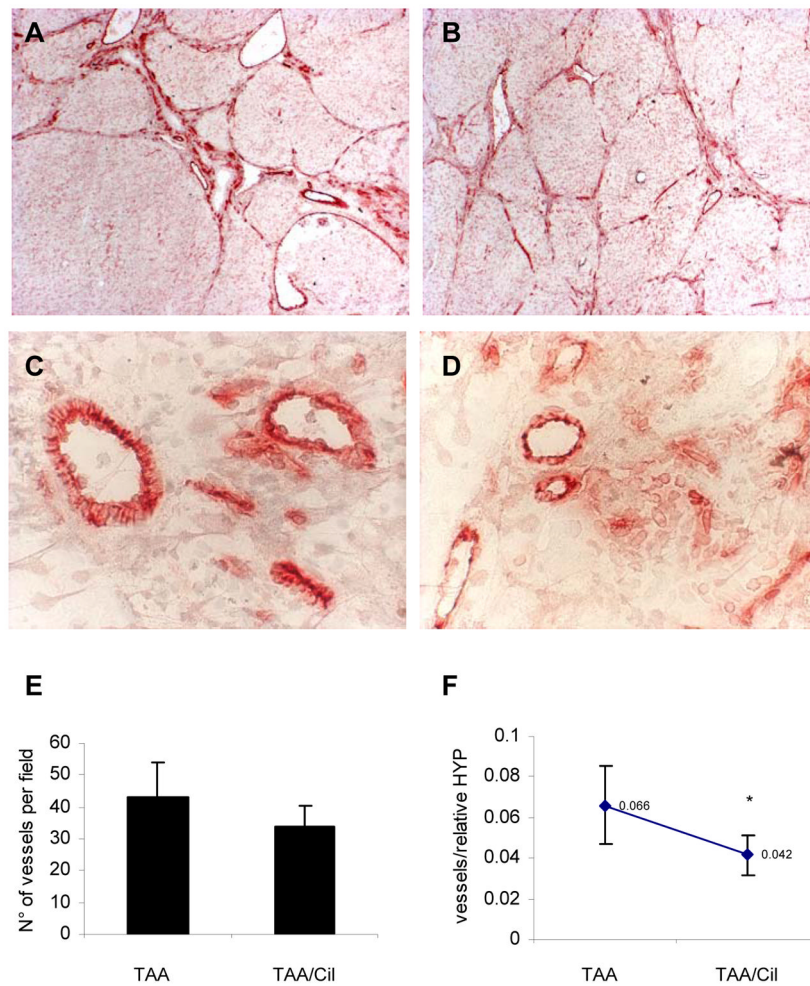
Fig.4. CD31 immunohistochemistry on livers of rats with TAA-induced fibrosis treated with/ without Cilengitide

(**A**) TAA-R (n=7, magnification 10x); (**B**) TAA-R + Cilengitide 30mg/kg/day 8w (n=8) (10x); (**C**) and (**D**), magnifications of (A) and (B), respectively (40x). (**E**) Quantification of angiogenesis. Calculation of CD31-positive vessels was performed in four areas from each liver section using light microscopy (magnification 10x) and is expressed as a number of vessels per field (means±SD). (**F**) Vessel number per fibrotic area is expressed as the ratio of vessels to relative hepatic HYP (means±SD), *p<0.05 vs TAA-R group.
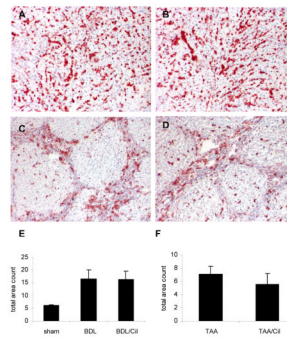
Fig.5. CD68 immunohistochemistry for macrophages/Kupffer cells on livers of rats with BDL and TAA-induced fibrosis treated with/without Cilengitide
(**A**) BDL 6w (n=8); (**B**) BDL 6w + Cilengitide 30mg/kg/day 5w (n=9); (**C**) TAA-R 8w (n=7); (**D**) TAA-R + Cilengitide 30mg/kg/day 8w (n=8). Morphometry of CD68 positive cells in (**E**) BDL and (**F**) TAA-induced fibrosis. Quantification of staining in each liver section was performed using Metamorph software and is expressed as total area count (means±SD).
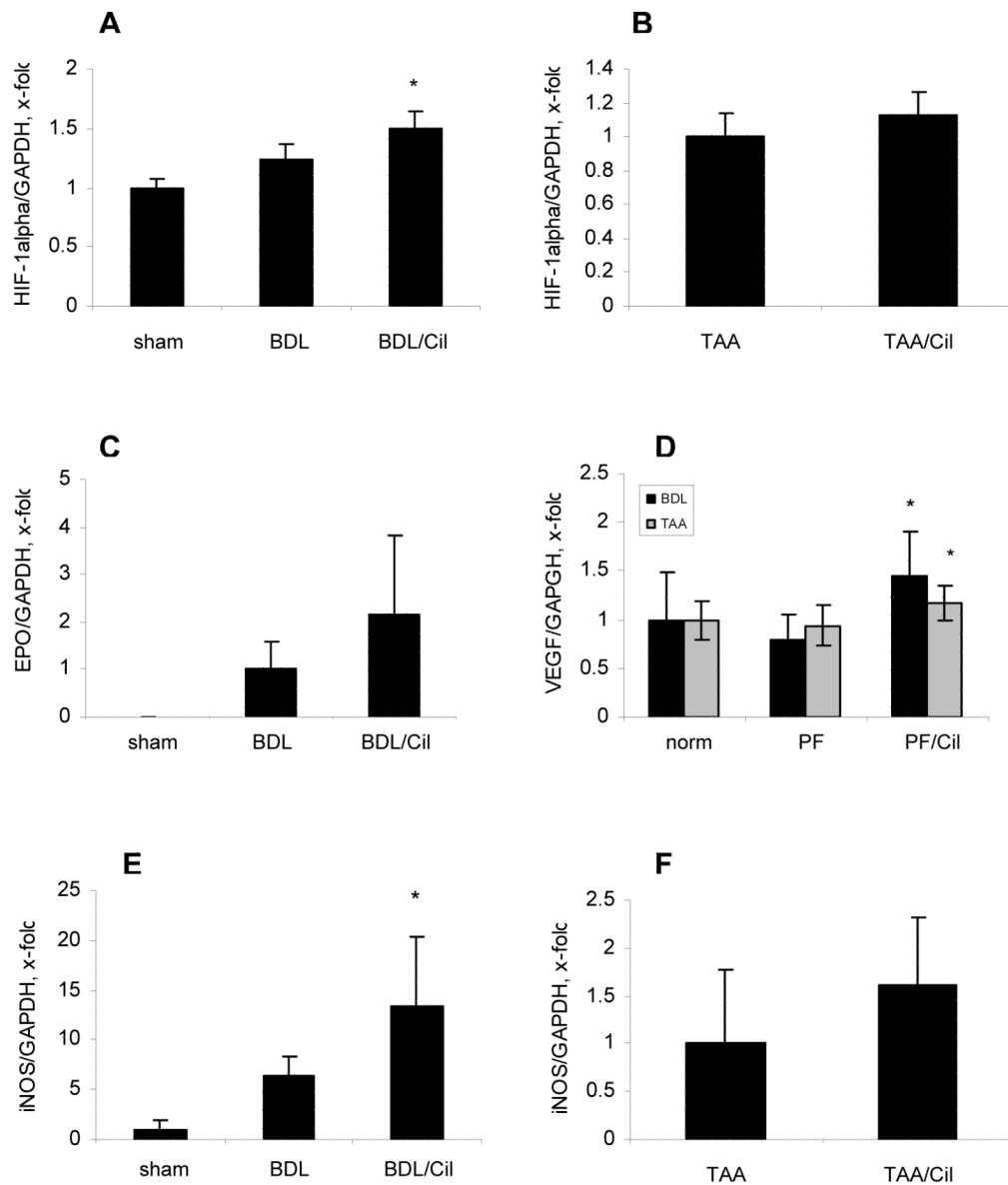
Fig.6. Upregulation of hypoxia-inducible genes in livers of fibrotic rats treated with Cilengitide
Hepatic expression of HIF-1α (**A,B**), EPO (**C**), VEGF (**D**) and iNOS (**E, F**) transcripts in
rats with BDL and TAA-induced fibrosis. Transcripts were quantified by TaqMan PCR,
normalized to GAPDH and expressed as x-fold change (means±SD). PF – peak of fibrosis;
*p<0.05 vs the corresponding fibrosis control.

Table 1

A. Transcript levels of genes related to fibrosis in rats with BDL

Targeted genes	Sham (n=4)	BDL 6 w (n=8)	Cilengitide 5w (n=9)
PC-α1(I)	1 ± 0.41	11.8 ± 1.9	19.5 ± 6.8[*]
TIMP-1	1 ± 0.63	7.12 ± 2.14	13 ± 5.4[*]
MMP-13	1 ± 0.67	1.07 ± 0.41	1.6 ± 0.4[*]
αSMA	1 ± 0.25	3.99 ± 1.72	5.9 ± 3.6
TGFβ1	1 ± 0.11	5.31 ± 1.01	9.8 ± 3.9[*]
TGFβ2	1 ± 0.19	22.6 ± 8.9	45.7 ± 30.5
TIMP-2	1 ± 0.34	4.49 ± 0.09	6.5 ± 2.2[*]
CTGF	1 ± 0.03	1.48 ± 0.93	3.33 ± 2.6
PDGF-BB	1 ± 0.14	12.2 ± 5.91	32.3 ± 21.6
PDGFR-β	1 ± 0.01	2.88 ± 0.34	5.93 ± 3.08[*]
PAI-1	1 ± 0.28	9.35 ± 2.6	19.1 ± 8.2[*]

B. Transcript levels of genes related to fibrosis in rats with TAA-induced fibrosis

Targeted genes	TAA-R 8 w (n=7)	Cilengitide 8w (n=8)
PC-α1(I)	12.2 ± 4.4	19 ± 7.6[*]
TIMP-1	2.9 ± 1.54	4.72 ± 1.5[*]
MMP-13	0.31 ± 0.16	0.6 ± 0.37
αSMA	7.24 ± 0.18	6.94 ± 0.16
TGFβ1	6.7 ± 0.26	6.23 ± 0.2
TGFβ2	7.6 ± 3.6	11.5 ± 4.2
PDGFR-β	6.93 ± 0.21	6.6 ± 0.21
PDGF-BB	9.9 ± 0.21	9.57 ± 0.19
CTGF	13.9 ± 0.24	12.7 ± 0.24

[*] p≤0.05 vs fibrosis control

Table 2

A. Organ weights and parameters of liver injury and fibrosis in rats with BDL

Parameters	Sham (n=4)	BDL 6w (n=8)	Cilengitide 5w (n=9)
liver weight, g	14.55 ± 0.63	36.8 ± 3.62	36.25 ± 9.9
spleen weight, g	0.88 ± 0.05	3 ± 0.41	2.9 ± 0.92
total HYP (mg)	3.59 ± 0.2	24.5 ± 8.7	31.7 ± 11.5
ALT (IU/L)	73.3 ± 14.8	127.5 ± 18	109.8 ± 35.1
ALP (IU/L)	180.7 ± 17.6	484.6 ± 62.4	404.2 ± 88.1
AST (IU/L)	119.3 ± 38.6	534.6 ± 60.1	403.1 ± 154.3
GGT (IU/L)	< 5	11.42 ± 4.05	53.3 ± 25[*]
bilirubin (μM/L)	0.1 ± 0.01	7.3 ± 1.4	9.8 ± 3.1

B. Organ weights and parameters of liver injury and fibrosis in rats with TAA

Parameters	Control (n=4)	TAA-R 8w (n=7)	Cilengitide 8w (n=8)
liver weight, g	13.84 ± 0.22	22.4 ± 4.7	22.5 ± 1.67
spleen weight, g	0.89 ± 0.08	2.19 ± 0.62	2.29 ± 0.25
total HYP (mg)	3 ± 0.4	14.5 ± 4.8	19 ± 2.3
ALT (IU/L)	34 ± 4.85	61.1± 15.6	74.8 ± 14.9
ALP (IU/L)	206 ± 58.4	400.8 ± 115.08	448.6 ± 63.7
AST (IU/L)	78 ± 11.52	104.9 ± 48.4	124.3 ± 27.4
GGT (IU/L)	< 5	6 ± 3.13	14 ± 4.1[*]
bilirubin (μM/L)	0.13 ± 0.06	0.22 ± 0.07	0.18 ± 0.11

[*] p≤0.05 vs fibrosis control.